

Between Shapes, Using the Hausdorff Distance*

Marc van Kreveld Tillmann Miltzow Tim Ophelders Willem Sonke
Jordi L. Vermeulen

Abstract

Given two shapes A and B in the plane with Hausdorff distance 1, is there a shape S with Hausdorff distance $1/2$ to and from A and B ? The answer is always yes, and depending on convexity of A and/or B , S may be convex, connected, or disconnected. We show that our result can be generalised to give an interpolated shape between A and B for any interpolation variable α between 0 and 1, and prove that the resulting morph has a bounded rate of change with respect to α . Finally, we explore a generalization of the concept of a Hausdorff middle to more than two input sets. We show how to approximate or compute this middle shape, and that the properties relating to the connectedness of the Hausdorff middle extend from the case with two input sets. We also give bounds on the Hausdorff distance between the middle set and the input.

1 Introduction

For two sets A and B in \mathbb{R}^2 , we define the *directed Hausdorff distance* as

$$d_{\vec{H}}(A, B) := \sup_{a \in A} \inf_{b \in B} d(a, b),$$

where d denotes the Euclidean distance. The *undirected Hausdorff distance* is defined as

$$d_H(A, B) := \max(d_{\vec{H}}(A, B), d_{\vec{H}}(B, A)).$$

If A and B are closed sets then $d_H(A, B) = r$ is equivalent to saying that r is the smallest value such that $A \subseteq B \oplus D_r$ and $B \subseteq A \oplus D_r$, where \oplus denotes the Minkowski sum, and D_r is a disk of radius r centered at the origin. Recall that the Minkowski sum of sets A and B is the set $\{a + b \mid a \in A, b \in B\}$. In this paper we consider only closed sets, and therefore we can freely use this containment property.

The Hausdorff distance has been widely used in computer vision [15] and computer graphics [6, 12] for tasks such as template matching, and error computation between a model and its simplification. At the same time, the Hausdorff distance is a classic mathematical concept. Our research motivation is to study this profound concept from a new perspective. Algorithms to compute the Hausdorff distance between two given sets are available for many types of sets, such as points, line segments, polylines, polygons, and simplices in k -dimensional Euclidean space [3, 4, 7]. However, the question whether a polynomial-time algorithm exists to compute the Hausdorff distance between general semialgebraic sets remains open [14].

In this paper, we consider the natural problem of finding a set that lies “between” two or more input sets, in a Hausdorff sense. In Section 2 we investigate the Hausdorff middle of sets A and B ; this is a set that has minimum undirected Hausdorff distance to A and B . Differently put, it minimizes the maximum of four directed Hausdorff distances. We show that when the Hausdorff distance between A and B is assumed to be 1, there is always a Hausdorff middle that has Hausdorff distance $1/2$ to A and B , and this is the best possible. We relate the convexity of A and/or B to the convexity and connectedness of the Hausdorff middle, and study its combinatorial complexity.

*Research on the topic of this paper was initiated at the 4th Workshop on Applied Geometric Algorithms (AGA 2018) in Langbroek, The Netherlands, supported by the Netherlands Organisation for Scientific Research (NWO) under project no. 639.023.208. The second author is supported by the NWO Veni grant EAGER. The first and fifth authors are supported by the NWO TOP grant no. 612.001.651.



Figure 1: Hausdorff morphs between three shapes.

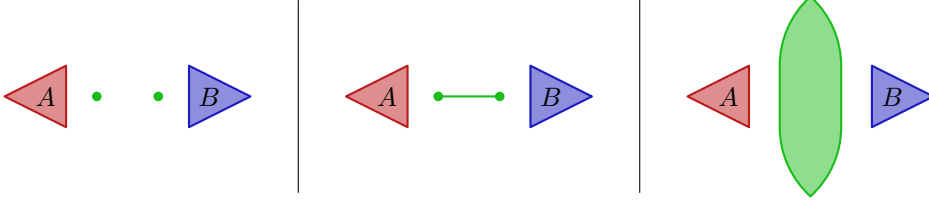


Figure 2: Three possible Hausdorff middles of A and B : two points, a line segment, and $S_{1/2}$.

We actually treat the middle more generally, by defining a class of sets that smoothly interpolate between A and B , giving a morph between them. Figure 1 shows two examples of such morphs. We prove that for two given intermediate shapes in the morph, the difference between the interpolation parameters bounds the Hausdorff distance between the shapes.

Algorithms for morphing, sometimes called *shape interpolation*, have been widely studied. A classical application is the reconstruction of a 3D object from 2D slices, a common problem in medical imaging. Many algorithms that solve this problem exist, based on straight skeletons [8, 10], curve matching and triangulations [9], and Delaunay triangulations [11]. When considering more abstract applications, a typical approach is to first transform each input shape into a canonical form, and then morph between those. Alt and Guibas [5] give an overview of this approach. Finally, work has been done to ensure the interpolation of two simple polygons is itself a simple polygon [19].

A common thread in all these algorithms is that they are based on computing some kind of correspondence between features of the input shapes, either by explicitly matching parts of the boundary, or by computing some geometrical structure (like a Voronoi diagram or a straight skeleton). In addition, most of these morphing algorithms interpolate only the boundary of the input shapes, and keep all intermediate shapes polygonal. Our approach does not require any correspondence between features of the input to be calculated. However, our approach is unusual in the sense that the intermediate shapes when morphing between e.g. two polygons are not necessarily polygons themselves.

In Section 3 we extend the results of Section 2 to Hausdorff middles of more than two sets and generalize several results. We assume that the maximum Hausdorff distance over all pairs of input sets is 1 and examine the smallest Hausdorff distance for a middle set. That is, given sets $\mathcal{M} = \{A_1, \dots, A_k\}$, we are interested in the value $\alpha(\mathcal{M}) = \min_S \max_{i=1, \dots, k} d_H(A_i, S)$. This value $\alpha(\mathcal{M})$ is no longer $1/2$, but depends on the input. For convex sets, we show that a value ≈ 0.608 can always be achieved and is sometimes necessary, whereas for non-convex sets a value of 1 may be required. For a given set of polygons with total combinatorial complexity n , we show that $\alpha(\mathcal{M})$ and the Hausdorff middle can be computed in $O(n^6)$ time, and, for any constant $\varepsilon > 0$, $(1 + \varepsilon)$ -approximated in $O(n^2 \log^2 n \log 1/\varepsilon)$ time. We note that other interpolation methods between two shapes do not have a natural generalization to a middle of three or more shapes.

Our proofs use three types of arguments. First, many of our arguments rely on simple manipulations of the formal definition of the Hausdorff distance. The second type of argument is of a topological nature. Using continuity and connectivity, we infer related properties to the output, by constructing topological structures or conclude that they cannot exist. The third type of argument uses 2-dimensional Euclidean geometry directly. We construct features, like vertices, edges and circular arcs, and argue about their existence, and give distance bounds. These arguments are often intricate and do not generalize. They are of particular value, as the 2-dimensional Euclidean plane is often the most interesting case in computational geometry.

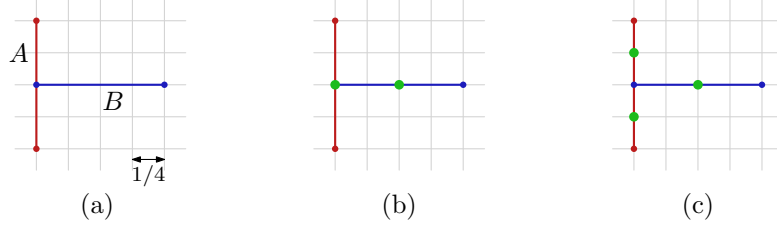


Figure 3: Two different minimal sets achieving minimal Hausdorff distance to A and B . Both the two green dots in Figure (b) and the three green dots in Figure (c) minimise the Hausdorff distance to A and B .

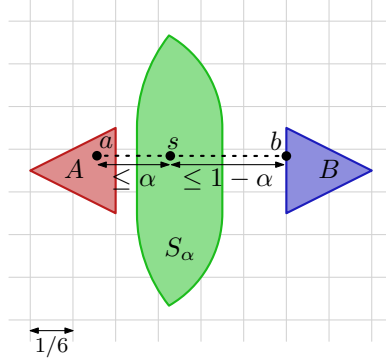


Figure 4: An arbitrary point $a \in A$ with its closest point b on B . The point s has distance at most α to a , and distance at most $1 - \alpha$ to b .

2 The Hausdorff middle of two sets

Consider two compact sets A and B in \mathbb{R}^2 ; we are interested in computing a *Hausdorff middle*: a set C that minimizes the maximum of the undirected Hausdorff distances to A and B . That is,

$$C \in \operatorname{argmin}_{C'} \max(d_H(A, C'), d_H(B, C')).$$

Note that there may be many such sets that minimize the Hausdorff distance; see Figure 2 for a few examples. It might seem intuitive to restrict C to be the minimal set that achieves this distance, but such a set is not necessarily unique, and the common intersection of all minimal sets is not a solution itself (see Figure 3). However, the maximal set is unique. Let $d_H(A, B) = 1$. Then

$$S(A, B) := (A \oplus D_{1/2}) \cap (B \oplus D_{1/2})$$

is the unique maximal set with Hausdorff distance $1/2$ to A and B (we prove this below in Lemma 2; see the right of Figure 2 for an example of what S looks like). Note that in the rest of the paper we omit the arguments and simply write S , as the arguments are always clear from context. We want to show that $d_H(A, S) \leq 1/2$ and $d_H(B, S) \leq 1/2$. In fact, we can prove a more general statement.

We define

$$S_\alpha(A, B) := (A \oplus D_\alpha) \cap (B \oplus D_{1-\alpha})$$

for $\alpha \in [0, 1]$, and we use $\operatorname{seg}(a, b)$ to denote the line segment connecting points a and b .

Theorem 1. *Let A and B be two compact sets in the plane with $d_H(A, B) = 1$. Then $d_H(A, S_\alpha) = \alpha$ and $d_H(B, S_\alpha) = 1 - \alpha$.*

Proof. We first show that $d_H(A, S_\alpha) \leq \alpha$. The proof for $d_H(B, S_\alpha) \leq 1 - \alpha$ is analogous and therefore omitted. We will infer $d_H(A, S_\alpha) \leq \alpha$ from $d_{\vec{H}}(A, S_\alpha) \leq \alpha$ and $d_{\vec{H}}(S_\alpha, A) \leq \alpha$; thereafter we will show equality.

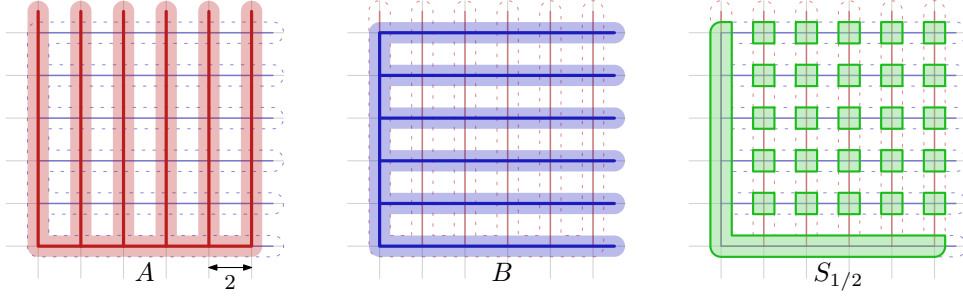


Figure 5: Sets A and B for which $S_{1/2}$ is disconnected. The shaded areas around A and B represent $A \oplus D_{1/2}$ and $B \oplus D_{1/2}$, respectively.

Consider any point $a \in A$; by our assumption that $d_H(A, B) = 1$, there is a point $b \in B$ with $d(a, b) \leq 1$; see Figure 4. Now consider a point $s \in \text{seg}(a, b)$ with $d(a, s) \leq \alpha$ and $d(b, s) \leq 1 - \alpha$; clearly this point must be in S_α , as it is contained in both $A \oplus D_\alpha$ and $B \oplus D_{1-\alpha}$, and it has $d(a, s) \leq \alpha$. As this works for every $a \in A$, it holds that $d_{\bar{H}}(A, S_\alpha) \leq \alpha$. The fact that $d_{\bar{H}}(S_\alpha, A) \leq \alpha$ follows straightforwardly from S_α being a subset of $A \oplus D_\alpha$. Thus, $d_H(A, S_\alpha) \leq \alpha$.

To show equality, assume that the Hausdorff distance between A and B is realized by a point $\hat{a} \in A$ with closest point $\hat{b} \in B$, at distance 1. Consider the point $\hat{s} \in \text{seg}(\hat{a}, \hat{b})$ with $d(\hat{a}, \hat{s}) = \alpha$ and $d(\hat{b}, \hat{s}) = 1 - \alpha$. As observed, $\hat{s} \in S_\alpha$. Since \hat{s} is the closest point of S_α to \hat{a} , and \hat{b} is the closest point of B to \hat{s} , equality follows. \square

Lemma 2. S_α is the maximal set that satisfies $d_H(A, S_\alpha) = \alpha$ and $d_H(B, S_\alpha) = 1 - \alpha$.

Proof. Consider any set T for which we have $d_{\bar{H}}(T, A) \leq \alpha$ and $d_{\bar{H}}(T, B) \leq 1 - \alpha$. As $A \oplus D_\alpha$ contains all points with distance at most α to A , we have that $T \subseteq A \oplus D_\alpha$; similarly, we have that $T \subseteq B \oplus D_{1-\alpha}$. By the definition of S_α , this implies that $T \subseteq S_\alpha$. As this holds for any T , we conclude that S_α is maximal. \square

2.1 Properties of S_α

In this section, we study the convexity and connectedness of S_α . Recall that a set $A \subseteq \mathbb{R}^2$ is convex if for any two points $a, b \in A$, the segment $\text{seg}(a, b)$ between them is completely contained in A . Also, recall that a set $A \subset \mathbb{R}^2$ is connected if for any two points $a, b \in A$, there exists a continuous curve $c : [0, 1] \rightarrow A$ such that $c(0) = a$ and $c(1) = b$. This type of connectedness is known as path-connectedness, but we use the term connected for simplicity. We observe the following properties:

1. If A and B are convex, S_α is convex;
2. If A is convex and B is connected, S_α is connected;
3. For some connected sets A and B , S_α is disconnected.

Property 1 is straightforward: the Minkowski sum of A and B with a disk is convex, and the intersection of convex objects is itself also convex. The example in Figure 5 demonstrates Property 3; in fact, *any* Hausdorff middle will be disconnected for those input sets.

The next lemma establishes Property 2.

Lemma 3. Let A and B be two connected regions of the plane with Hausdorff distance 1, and A convex. Then $S_\alpha = (A \oplus D_\alpha) \cap (B \oplus D_{1-\alpha})$ is connected for any $\alpha \in [0, 1]$.

Proof. See Figure 6 for an illustration. Because A is convex, there is a continuous map $\rho : B \rightarrow A$ that maps each point of B to a closest point (within distance 1) in A . For $b \in B$, let $\rho_\alpha(b) = \alpha\rho(b) + (1 - \alpha)b$. We have that $\rho_\alpha : B \rightarrow S_\alpha$ is also continuous.

Now take any two points s and s' in S_α ; respectively, they have points b and $b' \in B$ within distance $1 - \alpha$. The segments between s and $\rho_\alpha(b)$ and between s' and $\rho_\alpha(b')$ lie completely in S_α . Take a continuous curve π from b to b' inside B . The image of π under ρ_α connects $\rho_\alpha(b)$ to $\rho_\alpha(b')$ within S_α , so s and s' are connected inside S_α . \square

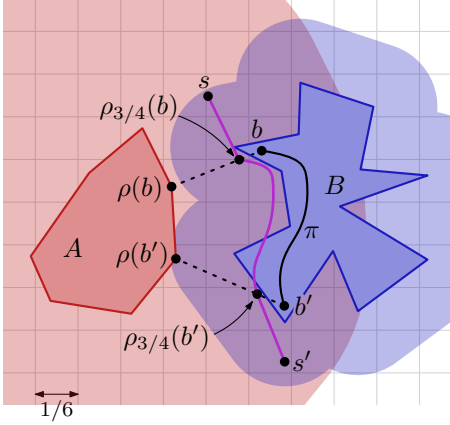


Figure 6: Illustration of the proof showing that S_α is connected if A is convex (sketched for $\alpha = 3/4$). The shaded areas around A and B represent $A \oplus D_{3/4}$ and $B \oplus D_{1/4}$, respectively, so that the doubly-shaded area is $S_{3/4}$.

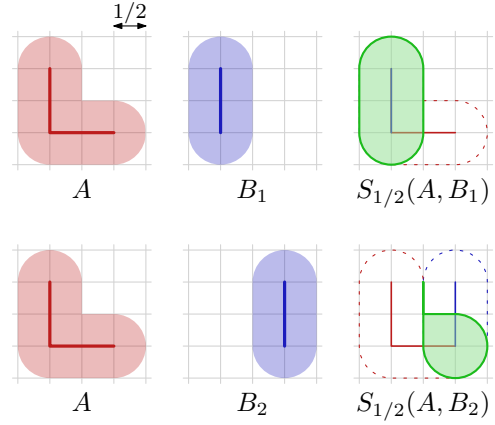


Figure 7: Although B_2 is a translate of B_1 , the middle set between A and B_2 is not a translate of the middle set between A and B_1 .

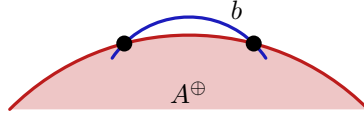


Figure 8: When $\alpha \geq 1 - \alpha$, an arc b of ∂B^\oplus (blue) can only intersect ∂A^\oplus (red) twice.

We note that S_α may contain holes. Furthermore, S_α is not shape invariant when B is translated with respect to A . For example, let A be the union of the left and bottom sides of a unit square and let B_1 and B_2 be the left and right sides of that same unit square. Then $(A \oplus D_{1/2}) \cap (B_1 \oplus D_{1/2})$ is not a translate of $(A \oplus D_{1/2}) \cap (B_2 \oplus D_{1/2})$. See Figure 7; note that $d_H(A, B_1) = d_H(A, B_2)$.

2.2 Complexity of S_α

In this section, we describe the complexity of S_α in terms of the number of vertices, line segments, and circular arcs on its boundary, for several types of polygonal input sets. Recall that ∂A denotes the boundary of set A .

Lemma 4. *Let A be a convex polygon with n vertices and B a simple polygon with m vertices. Then ∂S_α consists of $O(n + m)$ vertices, line segments and circular arcs, and this bound is tight in the worst case.*

Proof. For brevity we let $A^\oplus = A \oplus D_\alpha$ and $B^\oplus = B \oplus D_{1-\alpha}$.

There is a trivial worst-case bound of $\Omega(n + m)$ by taking $\alpha = 0$ or $\alpha = 1$, as $S_0 = A$ and $S_1 = B$. Note that if the boundaries of A^\oplus and B^\oplus would consist of only line segments, the upper bound is easy to show: A^\oplus is convex, and its boundary can therefore intersect each segment of ∂B^\oplus at most twice, making ∂S_α consist of (parts of) segments from ∂A^\oplus and ∂B^\oplus and at most $O(m)$ intersection points. The problem is that ∂A^\oplus and ∂B^\oplus also contain circular arcs, in which case ∂A^\oplus may intersect an arc of ∂B^\oplus $\Omega(n)$ times.

To show an upper bound of $O(n + m)$, we distinguish two cases. In the first case, we assume $\alpha \geq 1 - \alpha$. Note that in this case, the circular arcs that are part of the boundary of A^\oplus have a radius larger or equal to those of B^\oplus . Additionally, ∂A^\oplus is smooth and is an alternating sequence of circular arcs and segments, as A is convex. In this case, we do in fact have that any line segment or circular arc b of ∂B^\oplus can intersect ∂A^\oplus at most twice. Consider two intersection points of b with ∂A^\oplus : as the curvature of ∂A^\oplus is at most that of b , there can never be another intersection point between these two, or we would violate the convexity of A^\oplus . See Figure 8 for an illustration of this case.

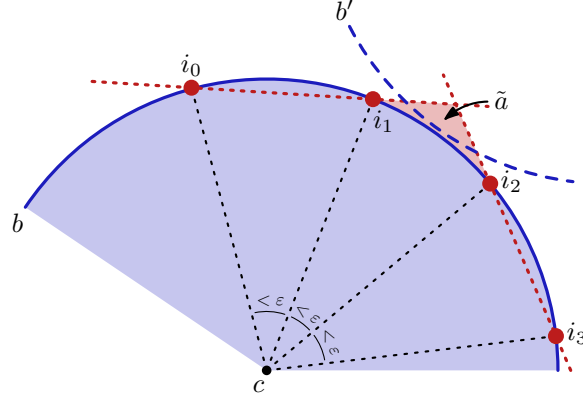


Figure 9: When $\alpha < 1 - \alpha$, a single arc b of ∂B^\oplus , shown in blue, can have many intersections with ∂A^\oplus , but no other arc b' , shown as a dashed blue arc, can have many intersections with the same part of ∂A^\oplus . The intersections of b with ∂A^\oplus are shown in red.

For the second case, we assume $\alpha < 1 - \alpha$. We charge all the intersections to the arcs and edges of ∂A^\oplus and ∂B^\oplus . Each edge of ∂B^\oplus can intersect ∂A^\oplus at most twice, as A^\oplus is convex, so there can be at most $O(m)$ such intersections. Similarly, for arcs of ∂B^\oplus that intersect ∂A^\oplus at most three times, there can be at most $O(m)$ intersections in total. It remains to consider the arcs of ∂B^\oplus that intersect ∂A^\oplus more than three times.

Let b be such an arc of ∂B^\oplus . Consider any quadruple of consecutive intersection points i_0, i_1, i_2, i_3 with ∂A^\oplus along b , see Figure 9, where the part of ∂A^\oplus between i_1 and i_2 that does not contain i_0 and i_3 is outside the disk supporting b . This part is denoted \tilde{a} ; note that \tilde{a} must contain at least one circular arc, denoted a . Notice that we consider all intersection points between ∂A^\oplus and b , except possibly for the first one or two and last one or two. These first and last ones can be charged to b , and this charge is at most four per arc b . Let c be the center of the supporting disk of b . If any of the angles $\angle i_0 c i_1$, $\angle i_1 c i_2$, or $\angle i_2 c i_3$, is larger than ε for some constant $\varepsilon > 0$, we again charge the intersection points i_1 and i_2 to b , and we have less than $360/\varepsilon$ of such charges. So we now assume that all three angles are at most ε . We charge the intersection points i_1 and i_2 to a , the arc of a disk that appears on \tilde{a} .

It remains to show that a is charged at most once. We can limit the distance by which \tilde{a} can protrude outside of b : as A^\oplus is convex, \tilde{a} cannot cross the line through i_0 and i_1 , nor the line through i_2 and i_3 . This restricts \tilde{a} to the shaded area in Figure 9. It is possible that \tilde{a} intersects a different arc b' of ∂B^\oplus in this shaded area. We observe that the disk that b' is a part of cannot contain the intersection points i_1 and i_2 , as otherwise those points would not be intersections of ∂A^\oplus and ∂B^\oplus . Now b' can intersect ∂A^\oplus at most twice, as more intersections would violate the convexity of A^\oplus . In particular, b' cannot intersect ∂A^\oplus four times, and hence b' cannot charge intersections on it to a . We conclude that a is charged only once. From this we conclude that there are at most $O(n + m)$ intersection points in total, and that ∂S_α therefore consists of at most $O(n + m)$ vertices, line segments and circular arcs. \square

Lemma 5. *Let A and B be two simple polygons of n and m vertices, respectively. Then ∂S_α consists of $O(nm)$ vertices, line segments and circular arcs, and this bound is tight in the worst case.*

Proof. The worst-case lower bound of $\Omega(nm)$ follows by taking A and B to be two rotated “combs”; see Figure 5. For $\alpha = 1/2$, S_α consists of $\Omega(nm)$ distinct components. The upper bound follows directly from the fact that $A \oplus D_\alpha$ and $B \oplus D_{1-\alpha}$ have complexities $O(n)$ and $O(m)$, respectively. Each individual arc and edge on the boundaries of $A \oplus D_\alpha$ and $B \oplus D_{1-\alpha}$ intersect at most a constant number of times, so we cannot have more than $O(nm)$ intersection points. \square

In fact, not just S_α , but *any* Hausdorff middle has complexity $\Theta(nm)$ for the example in Figure 5. S_α is maximal, so the components cannot be connected without changing the Hausdorff

distance to A or B , and other middles must have at least some point in every component of S_α to achieve Hausdorff distance $1/2$ to both A and B .

2.3 S_α as a morph

By increasing α from 0 to 1, S_α morphs from $A = S_0$ into $B = S_1$. (Examples of such morphs are presented in Figures 1 and 10.) The following lemma shows that this morph has a bounded rate of change.

Lemma 6. *Let S_α and S_β be two intermediate shapes of A and B with $d_H(A, B) = 1$ and $\alpha \leq \beta$. Then $d_H(S_\alpha, S_\beta) = \beta - \alpha$.*

Proof. We have $d_H(S_\alpha, S_\beta) \geq \beta - \alpha$ because, by the triangle inequality, $d_H(A, B) = 1 \leq d_H(A, S_\alpha) + d_H(S_\alpha, S_\beta) + d_H(S_\beta, B) \leq \alpha + d_H(S_\alpha, S_\beta) + 1 - \beta$.

It remains to show that $d_H(S_\alpha, S_\beta) \leq \beta - \alpha$. We show that $S_\beta \subseteq S_\alpha \oplus D_{\beta-\alpha}$; the proof that $S_\alpha \subseteq S_\beta + D_{\beta-\alpha}$ is analogous. Let p be some point in S_β . Then, by definition of S_β , there exist some points $a \in A$ and $b \in B$ such that $d(a, p) \leq \beta$ and $d(b, p) \leq 1 - \beta$. Let \bar{p} be the point obtained by moving p in the direction of a by $\beta - \alpha$. By the triangle inequality, we then have that $d(a, \bar{p}) \leq \beta - (\beta - \alpha) = \alpha$ and $d(b, \bar{p}) \leq (1 - \beta) + (\beta - \alpha) = 1 - \alpha$. This implies that $\bar{p} \in S_\alpha$. As p was an arbitrary point in S_β , and $d(p, \bar{p}) \leq \beta - \alpha$, we have that $S_\beta \subseteq S_\alpha \oplus D_{\beta-\alpha}$. So $d_H(S_\alpha, S_\beta) \leq \beta - \alpha$. \square

The lemma implies that, even though the number of connected components of S_α can change when α changes, new components arise by splitting and never ‘out of nothing’, and the number of components can only decrease through merging and not by disappearance.

The morph $\langle S_\alpha \mid \alpha \in [0, 1] \rangle$ from A to B has a consistent submorph property, formalized below.

Lemma 7. *If a morph from $A = S_0$ to $B = S_1$ contains a shape C , then the morph from A to C concatenated with the morph from C to B is the same as the morph from A to B : they contain the same collection of shapes in between and in the same order.*

Proof. Let α be the value such that $S_\alpha(A, B) = C$. We define $S'_\beta := (A \oplus D_\beta) \cap (C \oplus D_{\alpha-\beta})$ for $\beta \in [0, \alpha]$, giving the morph from A to C . We need to show that $S_\beta(A, B) = S'_\beta(A, C)$. The case for the morph from C to B is analogous and therefore omitted.

Let x be any point in $S_\beta(A, B)$. By definition it has a distance of at most β to A , and Lemma 6 establishes that it has distance at most $\alpha - \beta$ to C . This implies that $x \in S'_\beta(A, C)$. As this works for any point x , we have that $S_\beta(A, B) \subseteq S'_\beta(A, C)$. Now let x' be any point in $S'_\beta(A, C)$. By definition it has distance at most β to A , and distance at most $\alpha - \beta$ to some point $c \in C$. As $d_H(B, C) = 1 - \alpha$, by the triangle inequality x' must have distance at most $(\alpha - \beta) + (1 - \alpha) = 1 - \beta$ to some point in B . This shows $x' \in S_\beta(A, B)$. As this works for any point x' , we also have that $S'_\beta(A, C) \subseteq S_\beta(A, B)$. We conclude that $S_\beta(A, B) = S'_\beta(A, C)$. \square

As a corollary of this lemma, $\{\alpha \in [0, 1] \mid S_\alpha \text{ is convex}\}$ is a connected interval.

2.4 The cost of connectedness

For some applications, it might be necessary to insist that the middle shape is always connected. However, in the worst case, the cost of connecting all components of S_α can be that the Hausdorff distance of the resulting shape to A and B becomes 1. See Figure 11 for an example where this is the case. In fact, any connected shape has distance at least 1 for this example.

3 The Hausdorff middle of more than two sets

A natural question is whether the results from the previous section extend to more than two input shapes. There are several ways to formalise the notion of a Hausdorff middle between multiple shapes. Analogous to the case of two sets, we are interested in a middle shape that minimizes the maximum Hausdorff distance to each input set. Let $\mathcal{M} = \{A_1, \dots, A_m\}$ be a collection of m input shapes with largest pairwise Hausdorff distance 1. We define T_α as $\bigcap_i (A_i \oplus D_\alpha)$; the (maximal)

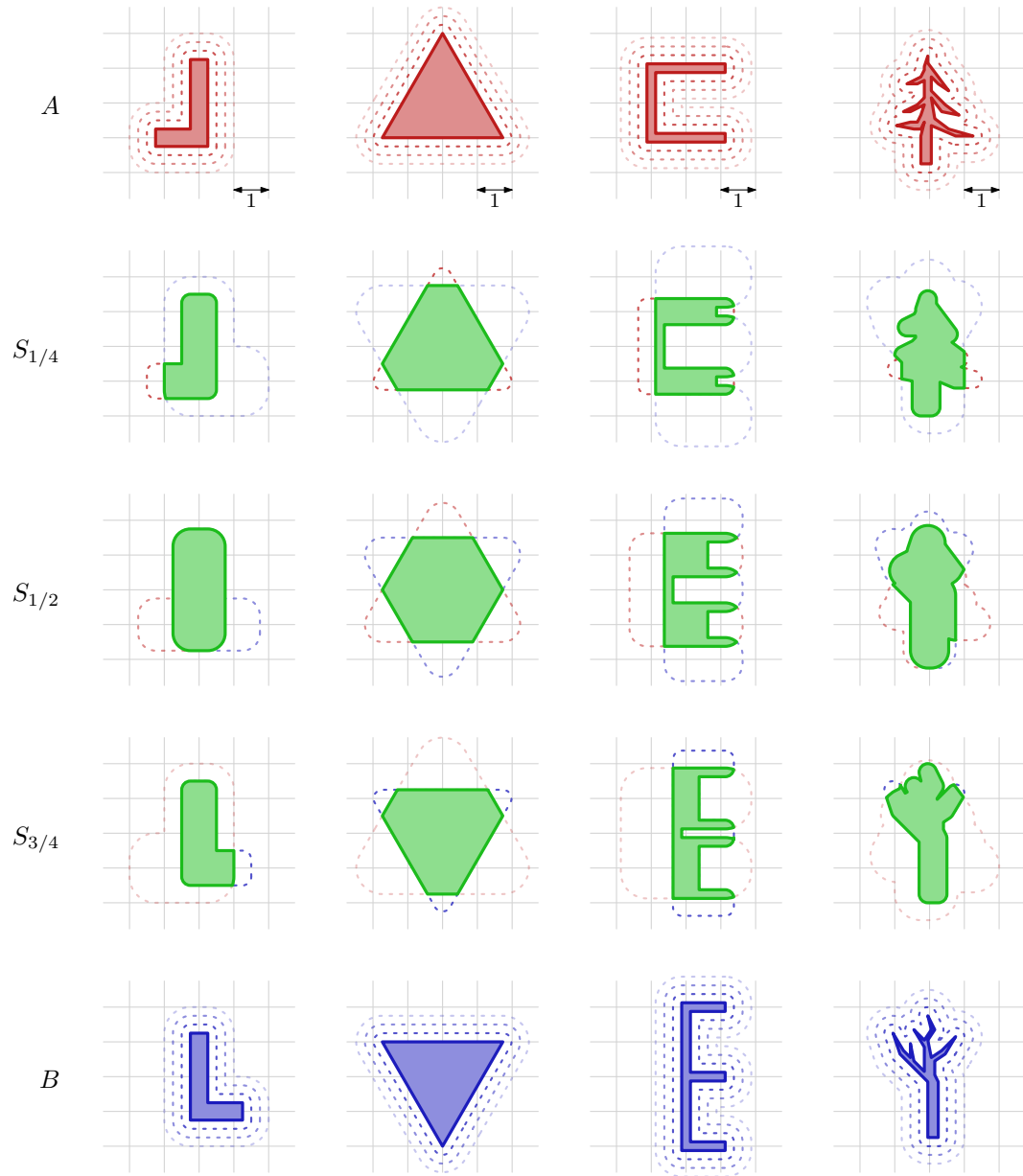


Figure 10: Some examples of morphs S_α between two shapes A and B .

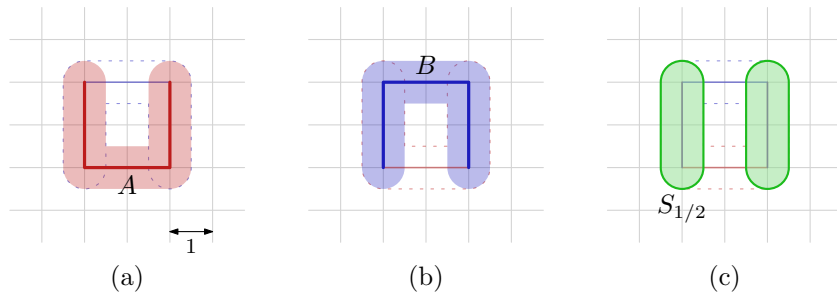


Figure 11: Figures (a) and (b) show the offsets of A , respectively B with distance $1/2$. Figure (c) shows the resulting $S_{1/2}$ in green. Any connected shape must cross the vertical middle line or stay on one side of it. In both cases, the Hausdorff distance doubles.

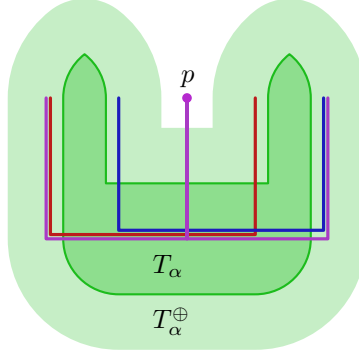


Figure 12: The pairwise Hausdorff distance in this construction is 1, and for any $\alpha < 1$, T_α^\oplus does not contain point p .

middle set is then given by the smallest value α for which $T_\alpha \oplus D_\alpha$ contains all input sets. We denote this smallest α by $\alpha(\mathcal{M}) := \min\{\alpha \mid \max_i d_H(A_i, T_\alpha) \leq \alpha\}$. If α is clear from the context, we use the notation A^\oplus to mean $A \oplus D_\alpha$.

In this section, we first study the largest possible $\alpha(\mathcal{M})$ for general and convex input. We then study some general properties of T_α with respect to connectivity and convexity. After this, we consider whether there is some subset of \mathcal{M} that requires the same value of α , and obtain a Helly-type property for convex input. Finally, we will give various algorithms to compute or approximate $\alpha(\mathcal{M})$ efficiently.

3.1 The largest $\alpha(\mathcal{M})$

In this section, we are interested in the largest possible value of $\alpha(\mathcal{M})$. We first discuss the general case and then study the case where all sets $A \in \mathcal{M}$ are convex. In both cases, we provide an exact answer. This section relies on some tedious calculations, which turn out to be easier if we do not normalize pairwise distances of our objects to 1.

As it turns out, for some inputs it may be the case that $\alpha(\mathcal{M}) = 1$; see Figure 12. Here, there can be no shape with Hausdorff distance less than 1 to all the input shapes, meaning any of the three input shapes can be chosen as “the middle”. Hence, for two input sets, we always have $\alpha(\mathcal{M}) = 1/2$, but for more input sets, the value depends on the input, and $\alpha(\mathcal{M})$ will be in $[1/2, 1]$. The example in Figure 12 requires non-convex sets, raising the question of what the range of $\alpha(\mathcal{M})$ can be when all A_i are convex.

If we have three convex sets that are points, and they form the corners of an equilateral unit-side triangle, then we can easily see that $\alpha(\mathcal{M}) = 1/\sqrt{3} \approx 0.577$ and the middle shape is exactly the point in the middle of the triangle.

An example with three line segments shown in Figure 13 surprisingly achieves (for $\lambda \approx 0.253135$, $\theta \approx 123.37^\circ$) a larger value $\alpha^* \approx 0.6068 = r$, which we call the *magic value*. Lemma 9 shows that no three convex sets achieve $\alpha(\mathcal{M}) > \alpha^*$. Thus the magic value is a tight upper bound for three convex sets.

We define the magic value as $\alpha^* = 1/z \approx 0.6068$, where the value of z is derived from Figure 14, and defined as $z := \min\{\lambda + 1 - \cos(2\theta) \mid \lambda \geq 0, \theta \in (90^\circ, 180^\circ), \text{ and } \lambda + 1 - \cos(2\theta) = \|(-\lambda \cot(2\theta) - \sin(2\theta) + \sin(\theta), \lambda - \cos(2\theta) + \cos(\theta))\|\} \approx 1.647986325231$ (at $\lambda \approx 0.253135$, $\theta \approx 123.37^\circ$, verified using Wolfram Cloud).

Lemma 8. *Let $\mathcal{M} = \{A_1, \dots, A_m\}$ be a collection of convex regions in the plane, and $\alpha := \alpha(\mathcal{M})$. There is some $A_i \in \mathcal{M}$ with $d_{\bar{H}}(A_i, T_\alpha) = \alpha$.*

Proof. By construction, we have $d_{\bar{H}}(T_\beta, A_i) \leq \beta$ for all i and all β . (Recall that this is equivalent to $T_\beta \subseteq A_i \oplus D_\beta$.) Moreover, if T_β is nonempty, then for any i , the map $\gamma \mapsto d_{\bar{H}}(T_\gamma, A_i)$ is continuous on the domain $[\beta, \infty)$, as T_γ changes continuously. We show that for some i , we have $d_{\bar{H}}(A_i, T_\alpha) = \alpha$. If instead $d_{\bar{H}}(A_i, T_\alpha) < \alpha$ for all i , then unless T_β is empty for all $\beta < \alpha$, we can decrease α , contradicting minimality of α . If instead α is the minimum value for which T_α is

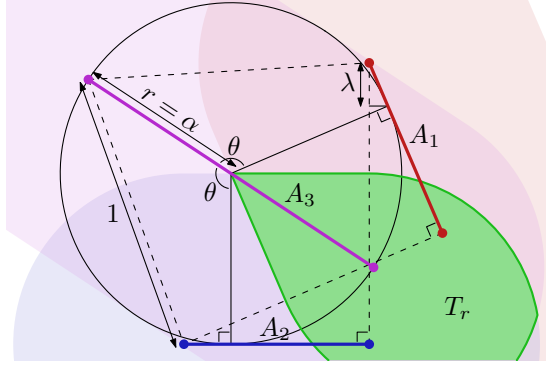


Figure 13: Three segments A_1 , A_2 , and A_3 . Of these, A_3 is the diameter of a circle with radius r ; the other two (A_1 and A_2) are tangent to the circle and are copies of one another reflected through A_3 , such that all pairwise Hausdorff distances are at most 1 (length of dashed segments). The top left vertex of A_3 is furthest (at distance r) from the middle set T_r (green), so $\alpha(\{A_1, A_2, A_3\})$ is the radius r of the circle.

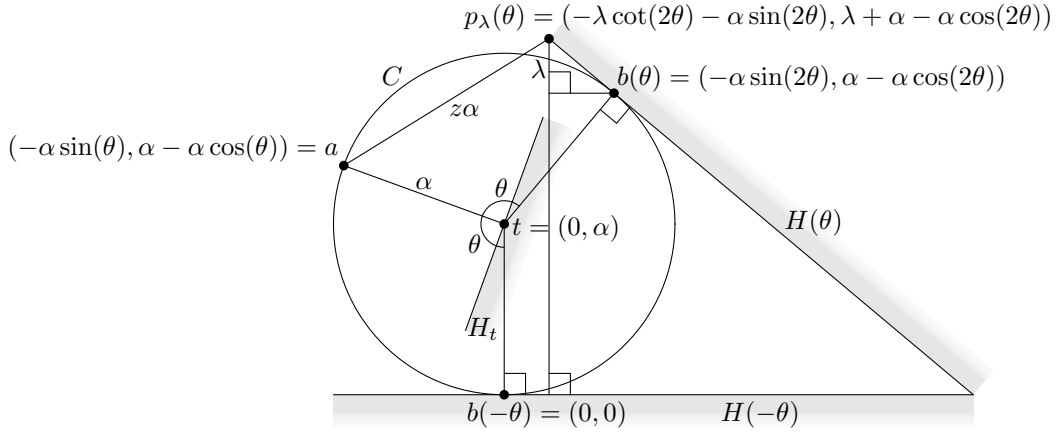


Figure 14: Derivation of the expression for z .

nonempty, then either $\alpha = 0$ and we are done because T_α contains all A_i , or $\alpha > 0$ and T_α has no interior (when viewed as a subset of the plane). Because T_α is the intersection of convex sets, it is convex. If it has no interior, it is either a segment or a point, and by convexity it must lie on the boundary of A_i^\oplus for some i , contradicting that $d_{\vec{H}}(A_i, T_\alpha) < \alpha$. \square

Lemma 9. Let $\mathcal{M} = \{A_1, A_2, A_3\}$ be convex regions in the plane. Let $\alpha := \alpha(\mathcal{M})$ and $d = \max_{i,j} d_H(A_i, A_j)$, then $d \geq \alpha/\alpha^*$ (equivalently $d \geq z\alpha$).

Proof. By Lemma 8, we have $d_{\vec{H}}(A_i, T_\alpha) = \alpha$ for some i . If x is a point, we will write $\vec{d}(x, \cdot)$ to denote $d_{\vec{H}}(\{x\}, \cdot)$. Without loss of generality assume that $d_{\vec{H}}(A_3, T_\alpha) = \alpha$ and $\vec{d}(a, T_\alpha) = d(a, t) = \alpha$ with $a \in A_3$ and $t \in T_\alpha$. Let $T = A_1^\oplus \cap A_2^\oplus \supseteq T_\alpha$. There is no point $t' \in T$ with $d(t', a) < \alpha$, since then $\vec{d}(t', A_3) < \alpha$, in which case $t' \in A_3^\oplus$ and therefore $t' \in T_\alpha$, contradicting that $d_{\vec{H}}(a, T_\alpha) = \alpha$. So t is a point in T closest to a and hence $\vec{d}(a, T) \geq \alpha$.

Assume that $\alpha > 0$ (otherwise we are done) and let H_t be the half-plane (not containing a) bounded by the line through t that is perpendicular to $\text{seg}(t, a)$, see also Figure 14. The set T is convex, as it is the intersection of convex sets. Therefore, if T contains a point p , then T also contains $\text{seg}(t, p)$. Since t is a point of T closest to a , no such segment intersects the open disk of radius α centered at a , and therefore $T \subseteq H_t$.

Let C be the circle of radius α centered at t . For the remainder of the proof, let $i \in \{1, 2\}$. Let b_i be a point of A_i closest to t . Then b_i lies on or inside C . If $b_i \neq t$, we can define the half-plane

H_i (not containing t) bounded by the line through b_i that is perpendicular to $\text{seg}(t, b_i)$. For $b_i \neq t$, we have by convexity of A_i and b_i being closest to t that $A_i \subseteq H_i$, so $\vec{d}(a, A_i) \geq \vec{d}(a, H_i)$. Without loss of generality, assume that $\vec{d}(a, H_i) < \alpha/\alpha^*$ (otherwise $d \geq d_H(A_3, A_i) \geq \vec{d}(a, A_i) \geq \alpha/\alpha^*$).

If $d(a, b_i) \geq 2\alpha$, then b_i lies diametrically opposite to a on C , but then $\vec{d}(a, H_i) \geq 2\alpha > \alpha/\alpha^*$, which is a contradiction, so $d(a, b_i) < 2\alpha$. Let $t_i \in A_i^\oplus$ be the midpoint of b_i and a , then $d(a, t_i) < \alpha = d(a, t)$. If $d(b_1, t) < \alpha$, then T contains a point interior to $\text{seg}(t, t_2)$, contradicting that $\vec{d}(a, T) \geq \alpha$. So b_1 and (analogously) b_2 lie on C .

Let θ_i be the clockwise angle $\angle atb_i \in (-180^\circ, 180^\circ)$. Define $b(\theta)$ to be the point on C for which θ is the clockwise angle $\angle atb(\theta)$, so that $b_i = b(\theta_i)$. Similarly, let $H(\theta)$ be the half-plane (not containing C) bounded by the line tangent to C at $b(\theta)$, so that $H_i = H(\theta_i)$. Assume without loss of generality that $|\theta_1| \geq |\theta_2|$ (otherwise relabel A_1 and A_2). If θ_1 and θ_2 are both positive or both negative, consider the circle of radius $\alpha/2$ centered at the midpoint of a and t . Then t_1 lies on the (shorter) arc of this circle connecting t_2 and t . This arc lies entirely in A_2^\oplus , so t_1 lies in T_α , which contradicts that there is no point $t' \in T$ with $d(t', a) < \alpha$. So assume without loss of generality that $\theta_2 \leq 0 \leq \theta_1$ (otherwise mirror all points). If $\theta_1 - \theta_2 < 180^\circ$, then T contains the segment between t and the midpoint of b_1 and b_2 . This segment does not lie in H_t , which contradicts that $T \subseteq H_t$. Moreover, if $\theta_1 - \theta_2 = 180^\circ$, then b_1 and b_2 are antipodal on C , so $d_H(A_1, A_2) \geq d_H(H(\theta_1), H(\theta_2)) = 2\alpha > \alpha/\alpha^*$. So consider the remaining case where $\theta_1 - \theta_2 > 180^\circ$.

In fact, it will turn out that in the worst case, $\theta_2 = -\theta_1$. Suppose that $p \in A_1 \subseteq H(\theta_1)$ is the point of A_1 closest to a . We have $d \geq d(a, p)$ and $d \geq \vec{d}(p, A_2) \geq \vec{d}(p, H(\theta_2))$. Moreover, since $-\theta_1 \leq \theta_2 < \theta_1 - 180^\circ$, the value of $\vec{d}(p, H(\theta))$ decreases as $\theta \in [-\theta_1, \theta_2]$ decreases. In particular, we have $\vec{d}(p, H(\theta_2)) \geq \vec{d}(p, H(-\theta_1))$. Since $|\theta_1| \geq |\theta_2|$, we have $\theta_1 \in (90^\circ, 180^\circ)$. Let $\lambda_p = \vec{d}(p, H(-\theta_1)) - \vec{d}(b(\theta_1), H(-\theta_1))$. If $\lambda_p < 0$, then $d(a, b(\theta_1)) < d(a, p)$, and p would not be a point of A_1 closest to a because the angle $\angle ab(\theta_1)p$ would be at least 90 degrees. Combining the above lower bounds, we obtain $d \geq \min\{\max\{d(a, p), \vec{d}(p, H(-\theta_1))\} \mid p \in H(\theta_1), \lambda_p \geq 0\}$. The right hand side of the above inequality is attained for some p on the boundary of $H(\theta_1)$. We parameterize such points p with parameters λ and θ_1 : let $p_\lambda(\theta_1)$ be the unique point on the boundary of $H(\theta_1)$ with $\vec{d}(p_\lambda(\theta_1), H(-\theta_1)) = \vec{d}(b(\theta_1), H(-\theta_1)) + \lambda$. The above inequality becomes $d \geq \min_{\lambda \geq 0} \max\{d(a, p_\lambda(\theta_1)), \vec{d}(b(\theta_1), H(-\theta_1)) + \lambda\}$.

We need to minimize this quantity over all values of $\lambda \geq 0$ and $\theta_1 \in (90^\circ, 180^\circ)$. We will show that it is minimized when its terms $d(a, p_\lambda(\theta_1))$ and $\vec{d}(b(\theta_1), H(-\theta_1)) + \lambda$ are equal. The point $p_\lambda(\theta_1)$, and hence the two terms, vary continuously in λ and θ_1 . For fixed θ_1 , both terms are convex as a function of λ . Therefore, for any fixed θ_1 , the function is minimized either when $\lambda = 0$, or the two terms are equal. As θ_1 approaches 180° , the first term approaches at least 2α (for any λ), and as θ_1 approaches 90° , the second term approaches at least 2α . Since the optimal value is less than 2α , there exists an optimal value of θ_1 . Assume for a contradiction that the terms are not equal in an optimal solution. Fix $\lambda = 0$, and consider the two terms as a function of θ_1 . For $\theta_1 \approx 90^\circ$ and $\lambda = 0$, we have $d(a, p_\lambda(\theta_1)) \approx \alpha < 2\alpha \approx \vec{d}(b(\theta_1), H(-\theta_1)) + \lambda$. Conversely for $\theta_1 \approx 180^\circ$ and $\lambda = 0$, we have $d(a, p_\lambda(\theta_1)) \approx 2\alpha > 0 \approx \vec{d}(b(\theta_1), H(-\theta_1)) + \lambda$. Hence, by the intermediate value theorem, the inequality as a function of θ_1 (with fixed $\lambda = 0$) is minimized when the terms are equal. We handled the case with $\lambda > 0$ above, so our inequality becomes $d \geq \min\{\vec{d}(b(\theta_1), H(-\theta_1)) + \lambda \mid \lambda \geq 0, \theta_1 \in (90^\circ, 180^\circ), \text{ and } d(a, p_\lambda(\theta_1)) = \vec{d}(b(\theta_1), H(-\theta_1)) + \lambda\}$. Following the derivation in Figure 14, this corresponds to $d \geq z\alpha = \alpha/\alpha^*$. \square

3.2 Convexity and connectedness of T_α

In this subsection, we use $\alpha := \alpha(\mathcal{M})$ for simplicity. Similar to Section 2.1, we examine the properties of T_α for different types of input. We arrive at straightforward generalizations of the results obtained for two sets.

1. If all A_i are convex, then T_α is convex.
2. If one of the A_i is connected and the rest are convex, then T_α is connected.

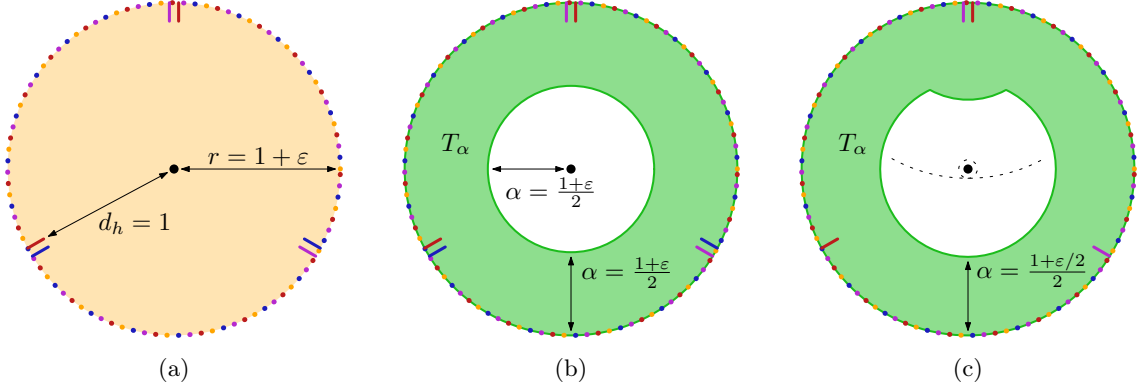


Figure 15: When the input sets are not convex, all sets may be necessary to realise the value of α . Figure (a) shows our input construction, along with the radius of the circle and the Hausdorff distance. Figure (b) shows that when all sets are present, the required value of α is $(1 + \varepsilon)/2$. Figure (c) shows that with the red set removed, the required value of α is reduced to $(1 + \varepsilon/2)/2$.

3. For some input where each A_i is connected, and at least two are not convex, T_α is disconnected.

Property 1 follows from the same argument as before: T_α is the intersection of convex sets, and therefore itself convex. Property 3 can be shown by extending the construction from Figure 5 with some other sets: if the intersection of two of the sets is not connected, adding more sets will not make T_α connected as long as the pairwise Hausdorff distance does not increase. We establish Property 2 with the following lemma.

Lemma 10. *Let $\mathcal{M} = \{A_1, \dots, A_m\}$ be a set of connected regions of the plane, with A_i convex for $i < m$. Then T_α is connected.*

Proof. Consider the set $T'_\alpha = \bigcap_{i=1}^{m-1} A_i^\oplus$. This set is convex, as it is the intersection of convex sets. Also note that by definition of T_α , A_m has directed Hausdorff distance at most α to T'_α . Let $A = T'_\alpha$ and $B = A_m$, normalised such that $d_{\vec{H}}(B, A) = 1$. We now apply Lemma 3 to A and B , using zero as the value for α . We obtain the result that $T_\alpha = T'_\alpha \oplus D_0 \cap A_m \oplus D_\alpha$ is connected. Note that the Hausdorff distance from A to B may be bigger than one, but this does not matter for the proof of Lemma 3. \square

3.3 Helly-type properties

An interesting question is whether there are any sets in the input that could be removed while maintaining the same optimal value of α . To make this precise, we need some definitions. We say a collection \mathcal{M} of m sets is d -sufficient, if there is a collection $\mathcal{M}_d \subset \mathcal{M}$ of d sets such that $\alpha(\mathcal{M}) = \alpha(\mathcal{M}_d)$.

Lemma 11. *For every m , there is a collection \mathcal{M} of m connected sets in the plane that is not $(m - 1)$ -sufficient.*

Proof. Figure 15 depicts a construction of four sets which are not 3-sufficient, which generalises to more sets. The example has one set that is a disk of radius $1 + \varepsilon$ (shown in orange in Figure 15(a)), and $m - 1$ sets that are circles on the boundary of this disk with $m - 1$ protrusions of some small length ε . These protrusions are evenly spaced along the boundary of the disk, and in each location there is a distinct set out of the $m - 1$ sets missing (each subset of size $m - 2$ is represented by some protrusion). In the example, we have protrusions containing the red and the blue set, the blue and the purple set, and the red and the purple set. This way, for the case where all sets are present (Figure 15(b)), the protrusions don't have any influence on T_α , meaning that $\alpha \geq (1 + \varepsilon)/2$ is required to let T_α^\oplus contain the entire disk. However, if we remove one set (other than the orange disk), there will be one protrusion where all sets are now present, meaning it will change the shape

of T_α . Because of this, the center of the disk will already be covered with a smaller value of α , namely $(1 + \varepsilon/2)/2$. This is shown in Figure 15(c): the dotted arc shows the dilation of the bump caused by the protrusion, which covers a part of the disk that would otherwise not be covered (shown as a dashed circle). Note that if we remove the orange disk, it is sufficient to use a value of $\alpha = \varepsilon/2$. Further note that with a minor adaptation, all sets become polygonal and simply connected. \square

We have shown that in general, we cannot remove any sets from the input while maintaining the same value of α . However, when all input sets are convex, we can show that there is always a subset of size at most three that has the same optimal value of α .

Lemma 12. *Let $\mathcal{M} = \{A_1, \dots, A_m\}$ be a collection of convex sets. Then there exists a subcollection $\mathcal{M}' \subseteq \mathcal{M}$ of size at most three such that $\alpha(\mathcal{M}) = \alpha(\mathcal{M}')$.*

Proof. Consider growing some value β from $1/2$ to 1 . At some point, T_β^\oplus contains all sets in \mathcal{M} . There are two ways in which this can happen: (1) T_β is non-empty for the first time, and immediately the condition holds, or (2) T_β grows, and its dilation now covers the last point of all sets in \mathcal{M} . As T_β is convex no new components can appear except for the first, and thus we have only those two cases.

In Case 1, T_β is either a segment or a point; otherwise, $T_{\beta'}$ would have been non-empty for some $\beta' < \beta$. If it is a segment, it is generated by two parallel edges of some $A_i, A_j \in \mathcal{M}$ such that we have $\alpha(\{A_i, A_j\}) = \alpha(\mathcal{M})$. If it is a point, it is the common intersection of the dilation of some number of sets from \mathcal{M} ; we argue that you can always pick three sets for which β is optimal. Let a be the single point in T_β ; consider the vectors \mathcal{V} perpendicular to the boundaries of the dilated input sets intersecting in this point. The vectors \mathcal{V} must positively span the plane:¹ otherwise, all vectors would lie in a common half-plane, and a would not be the first point to appear in T_β . As we are in the plane, there must be subset $\mathcal{U} \subset \mathcal{V}$ of three vectors that positively span the plane by themselves. The three corresponding sets $A_i, A_j, A_k \in \mathcal{M}$ satisfy $\alpha(\{A_i, A_j, A_k\}) = \alpha(\mathcal{M})$.

In Case 2, as our input sets are convex, T_β itself is also convex. Let $a \in A_i$ be one of the last points of \mathcal{M} to be covered by T_β^\oplus . As T_β^\oplus is convex, a must be on its boundary; let c be the piece of boundary curve a lies on. This piece of curve is either generated by the dilation of some boundary curve in T_β , or by the dilation of one of its vertices. If it's the dilation of a boundary curve, it can be traced back directly to boundary curve of some A_j , in which case A_i and A_j have Hausdorff distance 2β , and $\alpha(\{A_i, A_j\}) = \alpha(\mathcal{M})$ for any choice of k . If it can be traced back to a vertex of T_β , this vertex is generated by the intersection of the boundaries of some A_j^\oplus and A_k^\oplus , in which case we also have that $\alpha(\{A_i, A_j, A_k\}) = \alpha(\mathcal{M})$. \square

Combining the previous lemma with Lemma 9, we obtain the following result.

Theorem 13. *Let $\mathcal{M} = \{A_1, \dots, A_m\}$ be a collection of convex regions in the plane, and let $T_\alpha = \bigcap_i A_i^\oplus$. Then $\alpha(\mathcal{M})$ is at most the magic value $\alpha^* \approx 0.6068$.*

3.4 Algorithms

For any given collection of polygons $\mathcal{M} = \{A_1, \dots, A_m\}$, we want to compute $\alpha(\mathcal{M})$. We present two algorithms, a simple approximation algorithm and a more complex exact algorithm. They both use the same decision algorithm as a subroutine. To be precise, given a collection of sets \mathcal{M} and some α , the decision algorithm decides if $\alpha \leq \alpha(\mathcal{M})$. We first present an algorithm for the decision problem. Then we sketch how they are used in the approximation algorithm and the exact algorithm. We denote all vertices and edges of the A_i as *features* of \mathcal{M} .

Decision algorithm Assuming the input has total complexity n , we can test whether a given value of $\alpha \leq \alpha(\mathcal{M})$ as follows. Compute the intersection T_α of the dilations $A_1^\oplus, \dots, A_m^\oplus$ in $O(n^2 \log n)$ time, using the construction of an arrangement of straight and circular arcs [17, 20]. The set T_α will always have at most quadratic complexity, but it can be disconnected. Next we compute T_α^\oplus . We take every connected component T of T_α separately, compute T^\oplus , and then

¹We say $v_i \in \mathbb{R}^2$ *span the plane positively*, if for every point $p \in \mathbb{R}^2$ there are some numbers $a_i \in \mathbb{R}^+$ such that $\sum a_i v_i = p$.

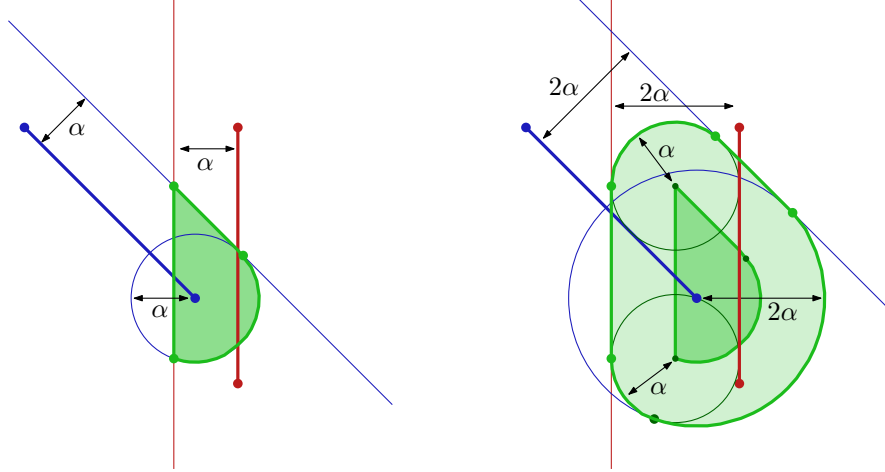


Figure 16: Left, two sets shown by red and blue line segments, and the construction of T_α from lines parallel to edges of \mathcal{M} and circles centered at vertices of \mathcal{M} . Right, construction of T_α^\oplus from lines at distance 2α from edges of \mathcal{M} , circles of radius 2α centered at vertices of \mathcal{M} , and circles of radius α centered at certain vertices of T_α .

compute their union. Since the connected components of T_α are disjoint and can be partitioned into $O(n^2)$ convex pieces, the Minkowski sums of these pieces with D_α form a set of pseudo-disks with total complexity $O(n^2)$, see [21]. It is known that such a union has $O(n^2)$ complexity and can be computed in $O(n^2 \log^2 n)$ time [1, 21]. Thus, we can compute T_α in $O(n^2 \log^2 n)$ time.

Note that $T_\alpha \subseteq A_i^\oplus$, by definition. It remains to test $A_i \subseteq T_\alpha^\oplus$, for each A_i . We test all those containments by a standard plane sweep [13] in $O(n^2 \log n)$ time. As soon as we find any proper intersection between an arc of $\partial(T_\alpha^\oplus)$ and some edge of some ∂A_i , we can stop the sweep and conclude that α needs to be larger. If there were no proper intersections of this type, there were only $O(n^2)$ events (and not $O(n^3)$), including the ones between edges of different ∂A_i . When there are no proper intersections, each shape A_i lies fully inside or outside T_α^\oplus . We can test this in $O(n^2 \log n)$ time (replace each A_i by a single point and then test by a plane sweep or planar point location [13]), and conclude that α must be larger or smaller than the one tested. Thus this decision algorithm takes $O(n^2 \log^2 n)$ total time.

Approximation algorithm The decision algorithm leads to a simple approximation algorithm to find a value of α that is at most a factor $1 + \varepsilon$ from the optimum. We can perform $\lceil \log 1/\varepsilon \rceil$ steps of binary search in the range $[1/2, 1]$, testing if T_α^\oplus contains all A_i using the above decision algorithm. This takes $O(n^2 \log^2 n \log 1/\varepsilon)$ time in total.

Exact computation We can compute an exact value of $\alpha(\mathcal{M})$ in polynomial time. To this end, we imagine a continuous process where we grow α from $1/2$, and keep track of T_α^\oplus . The first time (smallest α) T_α^\oplus covers all A_i , we have found the Hausdorff distance $\alpha(\mathcal{M})$ corresponding to the Hausdorff middle, and we can construct T_α explicitly as the Hausdorff middle. Such an approach is sometimes called *wavefront propagation* or *continuous Dijkstra*; it has been used before to compute Voronoi diagrams [13, 18], straight skeletons [2] and shortest paths on terrains [23]. This approach is combinatorial if there are finitely many events and we can determine each on time, before it occurs. Instead of explicitly maintaining T_α^\oplus when α grows, we will determine a polynomial-size set of critical α values that contains the sought one, and find it by binary search, using the decision algorithm described above.

The value $\alpha(\mathcal{M})$ that we aim to compute occurs when T_α^\oplus has grown just enough to cover all A_i . This can happen in three ways, roughly corresponding to a vertex of A_i becoming covered, an edge of A_i becoming covered at some point “in the middle”, or a hole of T_α^\oplus collapsing and disappearing interior to A_i . We call the vertices, edges, and arcs of \mathcal{M} and T_α^\oplus the *features* (of their boundaries). The three ways of covering all A_i , expressed in the features of \mathcal{M} and T_α^\oplus , are

now: (1) a feature of T_α^\oplus coincides with a vertex of some A_i , (2) a vertex of T_α^\oplus lies on a feature of some A_i , or (3) features of T_α^\oplus collapse and cause a hole of T_α^\oplus to disappear. In the last case, when that hole was inside some A_i , this can be the event where A_i is covered fully for the first time. In all cases, one, two, or three features of T_α^\oplus and zero or one feature of some A_i are involved, and at most three features in total. When three edge or circular arc features pass through a single point for some value of α , we say that these features are *concurrent*. Similarly, when an edge or circular arc passes through a vertex for some α , we say they are concurrent.

It can be that more than three features of T_α^\oplus pass through the point where, e.g., a hole in T_α^\oplus disappears, but then we can still determine this critical value by examining just three features of T_α^\oplus , and computing the α value when the curves of these three features are concurrent.

Let us analyze which features make up the boundary of T_α^\oplus , see Figure 16. There are four types: (1) straight edges, which are at distance 2α from an edge of \mathcal{M} , and parallel to it, (2) circular arcs of radius 2α , which are parts of circles centered at vertices of \mathcal{M} , (3) circular arcs of radius α , centered at a vertex of T_α , and (4) vertices where features of types (1)–(3) meet. Every one of the features of the boundary of T_α^\oplus is determined by one or two features of \mathcal{M} . In particular, each arc of type (3) is centered on an intersection point which is a vertex of T_α , of which there can be $\Theta(n^2)$ in the worst case (Figure 5). Depending on the type of intersection point, its trace may be linear in α , or may follow a low-degree algebraic curve (when the intersection has equal distance α to an edge and a vertex of \mathcal{M}).

Since any critical value can be determined as a concurrency of two (vertex and edge or arc) or three features (three edges or arcs) from \mathcal{M} and T_α^\oplus , and features of T_α^\oplus in turn are determined by up to two features of \mathcal{M} , every critical value depends on at most six features of the input \mathcal{M} . If we choose any tuple with up to six features of \mathcal{M} , and compute the α values that may be critical, we obtain a set of $O(n^6)$ values that contain all critical α values, among which $\alpha(\mathcal{M})$. We can compute this set in $O(n^6)$ time, as it requires $O(1)$ time for each tuple of up to six features of \mathcal{M} .

Theorem 14. *Let \mathcal{M} be a collection of m polygonal shapes in the plane with total complexity n , such that the Hausdorff distance between any pair is at most 1, and let $\varepsilon > 0$ be a constant. The Hausdorff middle of \mathcal{M} can be computed exactly in $O(n^6)$ time, and approximated within ε in $O(n^2 \log^2 n \log 1/\varepsilon)$ time.*

Parametric search could result in a faster exact algorithm, but for this one would need to express whether input features are close to a given S_α in terms of low-degree polynomials. This is nontrivial given that S_α as function of α varies in a complex manner.

4 Discussion and future research

We have defined and studied the Hausdorff middle of two planar sets, leading to a new morph between these sets. We also considered the Hausdorff middle for more than two sets. While we assumed that the input sets are simply connected, our definition of middle and the morph immediately generalize to more general sets, like sets with multiple components and holes. In this sense our definition of middle is very general. Other interpolation methods between shapes do not generalize to more than two input sets and cannot easily handle sets with multiple components.

There are many interesting open questions. For example, when both input sets are one-dimensional curves, is there a natural way to define a Hausdorff middle curve that is also 1-dimensional?

Besides the maximal middle set, there are other options for a Hausdorff middle. For example, we can choose S_α clipped to the convex hull of $A \cup B$, which is also a valid Hausdorff middle. In Figure 11, the green shape would be reduced to the part inside the square, which may be more natural. This Hausdorff middle can also be used in a morph.

Another interesting question could be if, for two shapes A and B , we can find a translation or rigid motion of A such that some measure on the Hausdorff middle (e.g. area, perimeter, diameter) is minimised.

For two or more shapes in the plane, we could also define a middle based on area of symmetric difference. Here we may want to average the areas for the middle shape, and possibly choose the middle that minimizes perimeter. This problem is related to minimum-length area bisection [22].

Similarly, for a set of curves, we could define a middle curve based on the Fréchet distance. This appears related to the Fréchet distance of a set of curves rather than just a pair [16].

References

- [1] P.K. Agarwal, J. Pach, and M. Sharir. State of the union (of geometric objects). Technical report, American Mathematical Society, 2008.
- [2] O. Aichholzer, F. Aurenhammer, D. Alberts, and B. Gärtner. A novel type of skeleton for polygons. *Journal of Universal Computer Science*, 1(12):752–761, 1995.
- [3] H. Alt, B. Behrends, and J. Blömer. Approximate matching of polygonal shapes. *Annals of Mathematics and Artificial Intelligence*, 13(3):251–265, Sep 1995.
- [4] H. Alt, P. Braß, M. Godau, C. Knauer, and C. Wenk. Computing the Hausdorff distance of geometric patterns and shapes. In Boris Aronov, Saugata Basu, János Pach, and Micha Sharir, editors, *Discrete and Computational Geometry - The Goodman-Pollack Festschrift*, pages 65–76. Springer, 2003.
- [5] H. Alt and L.J. Guibas. Discrete geometric shapes: Matching, interpolation, and approximation. In *Handbook of Computational Geometry*, pages 121–153. Elsevier, 2000.
- [6] Nicolas Aspert, Diego Santa-Cruz, and Touradj Ebrahimi. Mesh: Measuring errors between surfaces using the Hausdorff distance. In *Proc. IEEE International Conference on Multimedia and Expo*, volume 1, pages 705–708, 2002.
- [7] M.J. Atallah. A linear time algorithm for the Hausdorff distance between convex polygons. *Information Processing Letters*, 17(4):207 – 209, 1983.
- [8] G. Barequet, M.T. Goodrich, A. Levi-Steiner, and D. Steiner. Contour interpolation by straight skeletons. *Graphical Models*, 66(4):245–260, 2004.
- [9] G. Barequet and M. Sharir. Piecewise-linear interpolation between polygonal slices. *Computer Vision and Image Understanding*, 63(2):251–272, 1996.
- [10] G. Barequet and A. Vaxman. Nonlinear interpolation between slices. *International Journal of Shape Modeling*, 14(01):39–60, 2008.
- [11] J.-D. Boissonnat. Shape reconstruction from planar cross sections. *Computer Vision, Graphics, and Image Processing*, 44(1):1–29, 1988.
- [12] Paolo Cignoni, Claudio Rocchini, and Roberto Scopigno. Metro: measuring error on simplified surfaces. *Computer Graphics Forum*, 17(2):167–174, 1998.
- [13] M. de Berg, O. Cheong, M. van Kreveld, and M. Overmars. *Computational Geometry: Algorithms and Applications*. Springer, 3rd edition, 2008.
- [14] M.G. Dobbins, L. Kleist, T. Miltzow, and P. Rzażewski. $\forall\exists\mathbb{R}$ -completeness and area-universality. In *International Workshop on Graph-Theoretic Concepts in Computer Science*, pages 164–175. Springer, 2018.
- [15] M.-P. Dubuisson and Anil K. Jain. A modified Hausdorff distance for object matching. In *Proceedings of 12th IEEE International Conference on Pattern Recognition*, volume 1, pages 566–568, 1994.
- [16] A. Dumitrescu and G. Rote. On the Fréchet distance of a set of curves. In *CCCG*, pages 162–165, 2004.
- [17] H. Edelsbrunner, L. Guibas, J. Pach, R. Pollack, R. Seidel, and M. Sharir. Arrangements of curves in the plane—topology, combinatorics, and algorithms. *Theoretical Computer Science*, 92(2):319–336, 1992.

- [18] S. Fortune. A sweepline algorithm for Voronoi diagrams. *Algorithmica*, 2(1-4):153, 1987.
- [19] C. Gotsman and V. Surazhsky. Guaranteed intersection-free polygon morphing. *Computers & Graphics*, 25(1):67–75, 2001.
- [20] D. Halperin and M. Sharir. Arrangements. In C.D. Tóth, J. O’Rourke, and J.E. Goodman, editors, *Handbook of Discrete and Computational Geometry*, chapter 28, pages 723–762. Chapman and Hall/CRC, 3rd edition, 2018.
- [21] K. Kedem, R. Livne, J. Pach, and M. Sharir. On the union of Jordan regions and collision-free translational motion amidst polygonal obstacles. *Discrete & Computational Geometry*, 1(1):59–71, 1986.
- [22] E. Koutsoupias, C. H. Papadimitriou, and M. Sideri. On the optimal bisection of a polygon. *ORSA Journal on Computing*, 4(4):435–438, 1992.
- [23] J.S.B. Mitchell, D.M. Mount, and C.H. Papadimitriou. The discrete geodesic problem. *SIAM Journal on Computing*, 16(4):647–668, 1987.